TECHNICAL REPORT

Research and Technical Support for WIPP: Trivalent Actinide and Lanthanide Partitioning in Culebra Dolomite

Date submitted:

August 30, 2016

Principal Investigator:

Leonel E. Lagos, Ph.D., PMP®

Florida International University Collaborator:

Hilary P. Emerson, PhD, EI, Task Manager

Los Alamos National Laboratory Collaborators:

Timothy Dittrich, PhD
Donald Reed, PhD

Submitted to:

U.S. Department of Energy
Office of Environmental Management
Under Cooperative Agreement # DE-EM0000598

FIU | Applied Research Center
FLORIDA INTERNATIONAL UNIVERSITY

Table of Contents

Table of Figures

Table of Tables

1.0 Introduction

The U.S. Department of Energy is operating a nuclear waste disposal facility known as the Waste Isolation Pilot Plant (WIPP) approximately 26 miles east of Carlsbad, New Mexico. It was originally authorized by congress in 1979 for the "express purpose of providing a research and development facility to demonstrate the safe disposal of radioactive waste from defense activities and programs of the U.S. exempted from regulation by the NRC." It has been accepting transuranic waste from the defense nuclear weapons program since March of 1999. Transuranic waste is defined as waste with radionuclides having an atomic number greater than 92, a half-life greater than 20 years, and a concentration greater than 100 nCi/g (U.S.EPA 1993).

Unfortunately, the WIPP facility is not currently accepting waste. On February 5, 2014, a salt hauling truck caught fire underground leading to a complete evacuation and shutdown of the facility. Then, on February 14, an unrelated event occurred. An airborne release occurred due to failure of a waste container. Although no employees received a dose greater than the 10 mrem limit, the release was exacerbated by an inadequate ventilation system design. Offsite, a slight elevation in $^{239/240}$Pu and ^{241}Am was detected although well below levels that could cause a public or environmental hazard.

In order to initially begin operating the facility, a probabilistic performance assessment (PA) was completed to demonstrate compliance within the regulatory limits over 10,000 years (U.S.DOE 1996). Currently, many parameters are being reviewed and updated in anticipation of the re-opening of the facility to accept waste later this year. The initial storage capacity of the facility was reported to be 1.78×10^5 m^3 of contact handled transuranic waste (CHTRU) and 5100 m^3 of remote handled transuranic waste (RHTRU) (U.S.DOE 1995). As of February 2014, the WIPP had accepted 90,600 m^3 of CHTRU and 360 m^3 of RHTRU through 11,900 shipments.

Deep geologic disposal of radioactive waste at the WIPP includes multiple barriers for containment: (1) waste form, (2) waste container, (3) engineered barriers and (4) geologic barriers. The geologic barriers are the last barrier to release of contaminants. The WIPP is located 2160 feet below ground level within the Salado rock salt deposit. Notably, salt deposits are currently also under consideration for deep geologic disposal of high level radioactive waste in Gorleben,

Germany, due to their favorable properties (BMWI 2008, Spiegel 2010). Salt deposits are ideal formations for long-term disposal of radioactive waste because: (1) permeability is extremely low for liquids and gases (saline solutions within salt domes are just as old as themselves, ~200 million years); (2) high thermal conductivity allows for decay heat to dissipate; and (3) deposits creep and react to mechanical loads allowing for areas to seal themselves off with time.

The performance assessment (PA) modeling indicates that human intrusion by inadvertently drilling into a pressurized brine pocket and/or the repository itself provides the most likely pathway for significant release of radionuclides from the system (U.S.DOE 1996). These releases may occur by five mechanisms: (1) cuttings, (2) cavings, (3) spallings, (4) direct brine releases, and (5) long-term brine releases. It must be noted that the first four mechanisms could lead to an immediate release of radionuclides to the accessible environment. The most likely release pathway after human intrusion is through horizontal transport in the permeable layers of the Rustler formation located above the Salado formation (Figure 1). Within the Rustler formation, the Culebra dolomite member is the most transmissive geologic layer and, therefore, the most susceptible release pathway (Meigs, Beauheim et al. 1997, Perkins, Lucero et al. 1999).

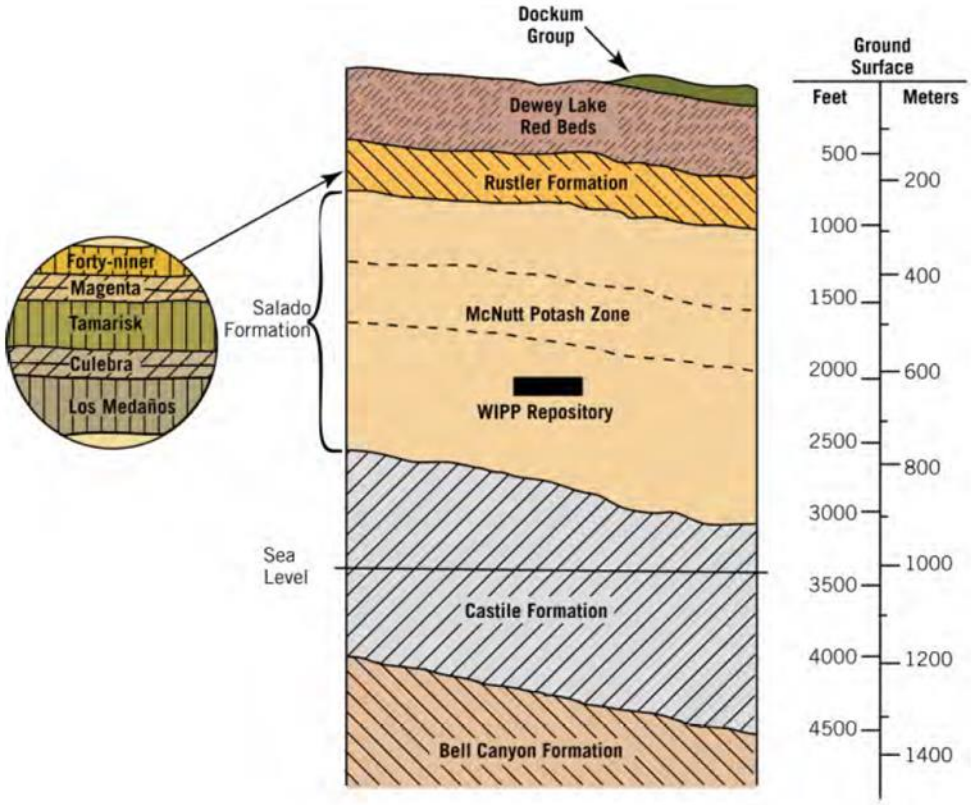

Figure 1. Geologic profile of the Waste Isolation Pilot Plant.

Because the Culebra dolomite is the most likely long-term release pathway, it has been the focus of multiple reports investigating actinide partitioning. Within the WIPP formation, the trivalent oxidation state is expected to dominate for both americium and plutonium with an assumption of 100% and 50% in the +3 oxidation state, respectively. However, the fate of trivalent actinides and lanthanides in this system is still not well understood due to their limited solubility and the limited range of conditions previously evaluated. For example, Perkins et al. conducted intact-core experiments but did not record breakthrough of Am(III) after many months of injection (Perkins, Lucero et al. 1999). In addition to the expected strong sorption of Am(III), it is likely that precipitation also occurred near the inlet.

Batch-type laboratory experiments have produced limited datasets describing trivalent actinide and lanthanide sorption to dolomite. Partitioning coefficients (K_ds) reported in the memo by Brush and Storz covered several different brine compositions related to the WIPP but did not report the pH for Am(III) K_ds and reported limited data for Nd(III) for atmospheric CO_2 in 0.05 M NaCl (Brush and Storz 1996). Moreover, Brady et al. used a limited residence time reactor setup but exceeded

Nd(III) solubility for pH 6-8 and reported only a limited pH range (3-6) for Am(III) for 0.05 and 0.5 M NaCl (Brady, Papenguth et al. 1999). However, applicable brines in the WIPP are on the order of 5.3 M (ERDA-6) and 7.4 M (GWB) (Lucchini, Borkowski et al. 2014). Overall, the range of K_ds reported previously spans the range from $10^{3.4}$ to 10^6 (Brush and Storz 1996, Brady, Papenguth et al. 1999, Perkins, Lucero et al. 1999).

Because there is insufficient historical data describing the sorption of trivalent actinides and lanthanides to Culebra dolomite, conservative assumptions were made for the WIPP PA. The final K_ds used for the PA for the WIPP were 20 to 400 mL/g for Pu(III) and Am(III) for deep brines (Brush and Storz 1996). However, these assumptions are based on reported K_ds for Am(III) and Pu(V) [not Pu(III)]. Therefore, it will be useful to accurately measure the partitioning of trivalent actinides and lanthanides in these systems in the event that risk assessment models are updated, conditions within the WIPP change, or human intrusion leads to a potential release.

2.0 Objectives

From February 14 through April 9, 2016, Hilary Emerson traveled to Carlsbad, NM as a visiting scientist to begin a new collaboration between the Carlsbad Environmental Monitoring and Research Center (CEMRC) and the Applied Research Center (ARC) at Florida International University (FIU) in support of the WIPP risk assessment activities. The overall objective of this task was to obtain sorption/desorption parameters for trivalent actinides and lanthanides (Nd and Am) to Culebra dolomite. Prior to the laboratory experiments, the Culebra dolomite was characterized by conventional techniques. Further, the work begun at CEMRC consisted of two (2) sets of experiments: laboratory batch sorption and mini columns. Both batch sorption and column experiments were utilized to receive the most accurate sorption parameters. Because of the expected strong sorption of Nd and Am, it is difficult to conduct batch experiments without artefacts due to sorption to vial walls, precipitation, etc. The mini column setup likely introduces fewer experimental artifacts and is more representative of environmental conditions but takes significantly more time experimentally. However, both techniques were conducted as a part of this collaboration and once the data collection is completed both will be compared with previous work.

3.0 Materials and Methods

3.1 Mineral Preparation and Characterization

Before experiments were conducted, Culebra dolomite mineral samples were crushed, cleaned and characterized. First, the dolomite rock samples were be crushed in an impact mortar and pestle and then washed and sieved. The 355 – 500 µm size fraction was utilized for all batch and column experiments. If the finer fractions were used for columns, it would likely clog. Therefore, the 355 – 500 µm size fraction was used for all experiments for consistency.

The following procedure was followed:

1. Lightly crush sample in an impact mortar and pestle
2. Sieve dry solid through No. 45, 100 and 200 size sieve
3. Remove largest size fraction (>500 µm) and re-crush
4. Continue steps and 2 and 3 until all of the solid has been processed through sieves
5. Rinse all solids with Milli-Q (>18 MΩ) H_2O
6. Dry ~24 hours at 40°C
7. Re-sieve all dry solids

The minerals within the Culebra dolomite samples were analyzed by a combination of x-ray diffraction (XRD) and scanning electron microscopy with energy dispersive x-ray spectroscopy (SEM-EDS). Bulk surface area was estimated through the Brunauer-Emmett-Teller (BET) method by the Mechanical Engineering Department at Florida International University (Micromeritics TriStar II 3020).

3.2 Batch Sorption Experiments

3.2.1 Batch Experimental Conditions

Experiments were conducted at variable solids (Culebra dolomite, 5, 25 and 100 g/L) with a 40 mL volume and pH of 8.5 – 9.5 to investigate the loading capacity and kinetic and equilibrium partitioning of Nd. Initial experiments were conducted with Nd to simplify the protocols without radiation safety hazards, although future experiments will include Am and Pu(III). Experiments were conducted with variable ionic strength 0.01 – 5 M (NaCl + 3 mM $NaHCO_3$). Further,

transport in the presence of ligands deemed applicable to the WIPP will also be considered for future experiments.

Nd was not added to the batch samples until the pH had been allowed to equilibrate (24-48 hours). The initial Nd concentration was 20 µg/L following initial experiments and geochemical modeling in order to remain below solubility within the chosen pH range (Figures 2 and 3). Controls were also conducted without the presence of the solid phase (Culebra dolomite) to account for sorption to vial walls and losses during pH adjustment. Further, a buffer of 3 mM $NaHCO_3$ was used to control pH. This bicarbonate concentration is close to the level predicted in equilibrium with atmospheric carbon dioxide.

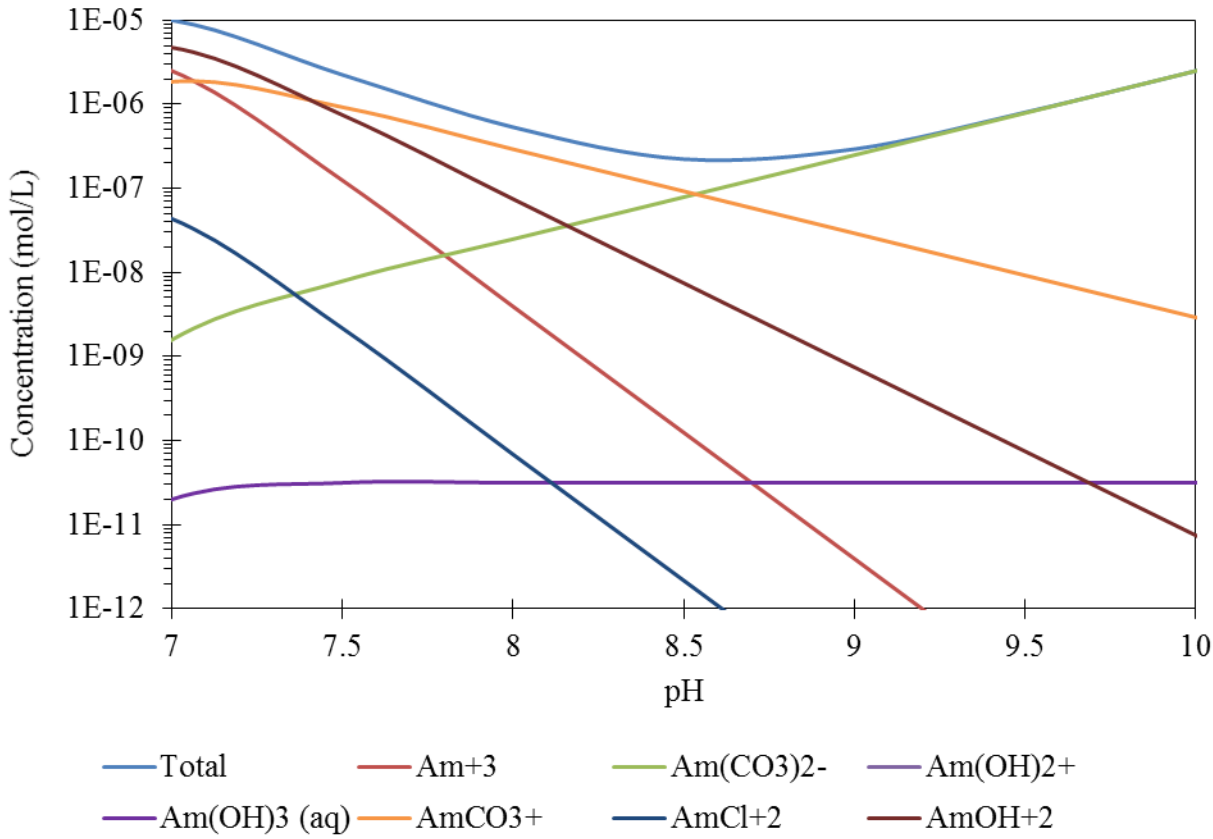

Figure 2. Am(III) speciation and solubility in the presence of atmospheric CO_2 and 0.01 M NaCl, modeled via Visual Minteq with standard database.

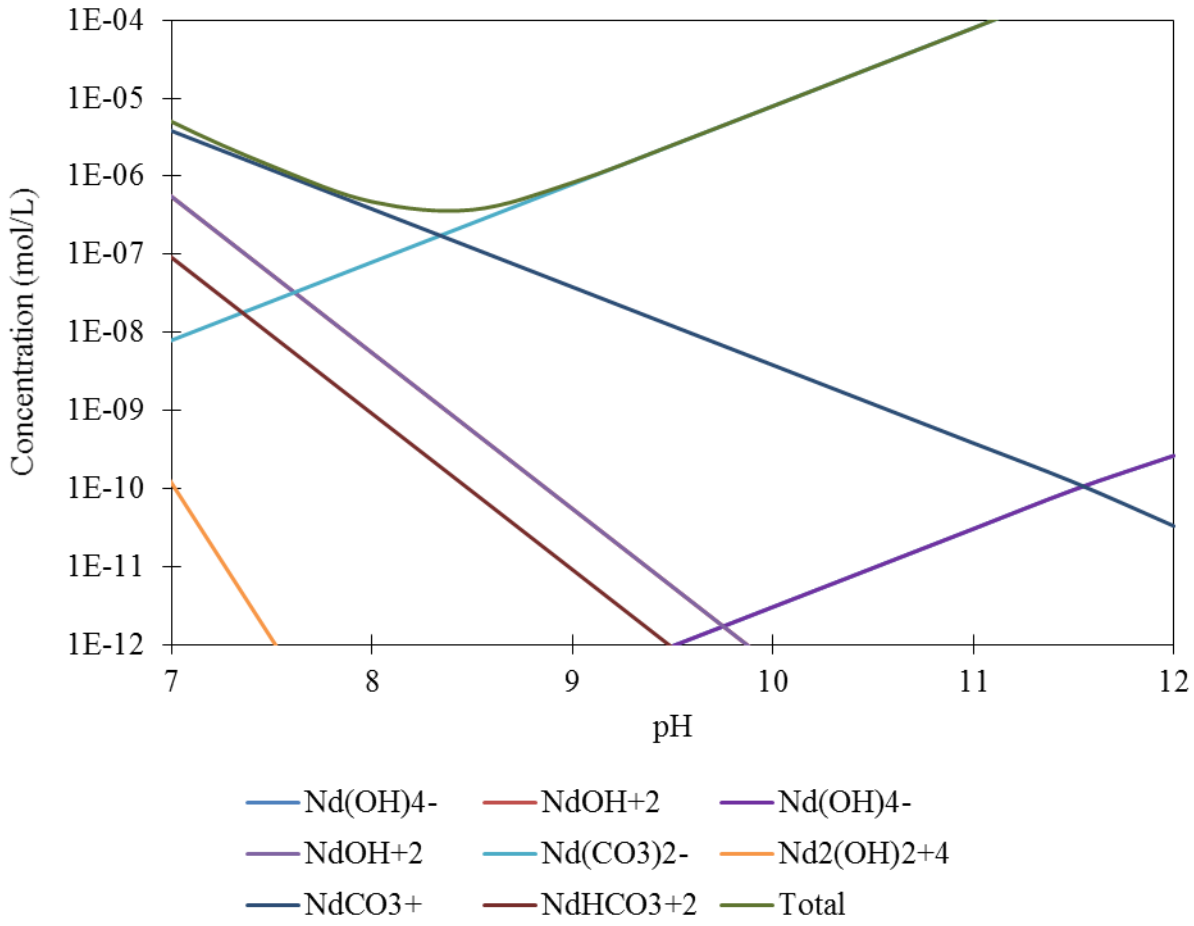

Figure 3. Nd(III) speciation and solubility in the presence of atmospheric CO_2 and 0.01 M NaCl, modeled via Visual Minteq with standard database.

Equilibrium experiments were allowed to equilibrate for 12 – 24 hours prior to sampling. This is expected to be sufficient as previous work has reported equilibrium within thirty seconds for Nd/Am (Brady, Papenguth et al. 1999) and with Eu/Sm sorption to calcite reported that equilibrium was reached within 24 hours (Zavarin, Roberts et al. 2005). However, kinetic experiments with variable time sampling from 15 minutes to 7 days were also conducted for comparison. All samples were analyzed by ICP-MS for Nd and major cations from ionic strength adjustment and dolomite dissolution (i.e. Na, Mg, Ca) following an acidification step in 2% HNO_3.

3.2.2 pC_{H+} Calculations

At high ionic strength conditions, there is a difference between pH (hydrogen ion activity) and pC_{H+} (hydrogen ion concentration). The pH reading of a glass electrode is not the same due to: (1) calibration with low ionic strength buffers, and (2) lack of data for activity coefficients. However,

a linear function has been shown to fit the data to predict pH and pC_{H+} and is in agreement with previous data (Rai, Felmy et al. 1995, Borkowski, Lucchini et al. 2009). In this work, pH and pC_{H+} were determined using corrections based on equation 1 as outlined previously (Borkowski, Lucchini et al. 2009). Borkowski has measured the K-value correction for 5 M NaCl as 0.82±0.03. The linear equation is shown in equation 2, where K is the correction factor and IS is the total ionic strength in mol/L. Although Rai et al. (1995) did not develop a linear correlation for the K-value, they did measure this factor at variable ionic strength in NaCl solutions and they correlate fairly well with the equation developed by Borkowski (2009).

$$pC_{H+} = pH + K \quad \text{Eqn. 1}$$

$$K = [IS \times -0.1868 \pm 0.0082] + 0.073 \quad \text{Eqn. 2}$$

3.2.3 Partitioning Coefficient and Kinetic Calculations

Equilibrium partitioning coefficients (K_d) were calculated per the equations below. Kinetic parameters were also estimated based on the equations outlined in Table 1. However, additional kinetic models will be examined in future work.

$$[An]_{sed} = \frac{([An]_{aq,i} - [An]_{aq,t})V_L}{m_{sed}} \quad \text{Eqn. 3}$$

where: $[An]_{sed}$= total concentration in sediment, µg/L (µg/$kg_{sediment}$)

$[An]_{aq,i}$= initial total aqueous concentration, µg/L (µg/L)

$[An]_{aq,t}$= total aqueous concentration at time, t, µg/L (µg/L)

V_L= sample liquid volume, L

m_{sed}= sample sediment mass, $kg_{sediment}$

The sediment water partitioning coefficient, K_d, will be calculated using the following equation:

$$K_d = \frac{[An]_{sed}}{[An]_{aq}} \quad \text{Eqn. 4}$$

Table 1. Kinetic Model Equations for Batch Sorption Experiments

Kinetic model	General Equation	Linear Equation	Plot
First-order	$C_t = C_o e^{-k_1 t}$	$ln[C_t] = ln[C_o] - k_1 t$	$ln[C_t]\ vs.\ t$
Second-order	$C_t = \frac{C_0}{1 + C_0 k_2 t}$	$\frac{1}{C_t} = \frac{1}{C_0} + k_2 t$	$\frac{1}{C_t}\ vs.\ t$

3.3 Mini Column Experiments

Miniature flow-through column experiments were designed based on previous work by Dittrich et al. and were used to better understand partitioning of Nd with the variable ionic strength and pH conditions described above for batch experiments (Dittrich and Reimus 2015, Dittrich, Ware et al. 2016). Columns are 1 cm in length with a porosity of 0.3 and equivalent pore volume of 0.44 mL as determined by mass. Further, the flow rate was 1.5 mL/hr (36 mL/day) for all columns which is equivalent to a 17.5 minute retention time within the column. Pictures are included in Figure 4 below for reference.

Figure 4. Image of mini column packed with dolomite (left) and image of fraction collector, syringe and column setup inside humidity chamber (right).

3.3.1 Preconditioning of Column

Preconditioning of the columns was done to equilibrate the mineral to the desired pH. The feed solution was pumped into the columns from the bottom to avoid the introduction of air bubbles and gravity effects. The effluent was collected and analyzed for pH and major cations (Ca, Mg, Na) and aqueous carbonate by ICP-MS. Once the effluent pH has reached that of the injection pH, then the column was pre-equilibrated and ready for the next step.

3.3.2 Sorption Experimental Procedure

Once the preconditioning of the column was complete, Nd was injected into the column from the bottom in the presence of 0.01 or 0.1 M total ionic strength (NaCl + 3 mM $NaHCO_3$). The effluent was collected at regular intervals (every 90 minutes) and analyzed for Nd via ICP-MS following acidification in 2% HNO_3. Select samples were also analyzed for major cations and filtered to check for particulate versus dissolved phases. This phase of the experiment will be terminated once the effluent contaminant concentration reaches the influent concentration (i.e., the column has been saturated with respect to the contaminant of concern). However, this column is still ongoing due to the high sorption capacity of dolomite for Nd.

3.3.3 Desorption Experimental Procedure

After the adsorption phase is complete, desorption of Nd will be studied by pumping pH-adjusted solutions without the contaminant of concern through the columns. Effluent samples will be collected at regular intervals until the pH of the effluent solution reaches the pH of the inlet solution. In order to conduct mass balance calculations, a final desorption step will be conducted by transferring the column material into a centrifuge tube with HNO_3 (pH 2-3). The concentration of the contaminant desorbed by the acid will be measured by ICP-MS. Preliminary data is presented for a column at 0.01 M total ionic strength. However, this column did not reach saturation. Desorption was checked on this column to test the procedures.

3.3.4 Retardation Factor Calculations

The potential for transport of the contaminant of concern will be quantified by calculating a retardation factor (R). A retardation factor is the ratio of the average linear velocity of groundwater to the velocity of the contaminant. Therefore, a conservative tracer should have a retardation factor of 1.0, but a contaminant that transports more slowly through a system than the tracer will have a retardation factor greater than 1.0. The retardation factor is estimated based on the mean residence

time τ (Eqn. 5) and can be expressed in terms of the aqueous volume V (Eqn. 6) (Clark 1996). The final retardation factor is calculated by dividing the aqueous volume, V_{aqu}, by the pore volume, V_{pore}, of the column. The pore volume is estimated for each column based on the difference in the dry, packed column mass and the wet column mass. Finally, the retardation factor (R) can be related to K_d by Eqn. 7 below. The ρ_b represents the bulk density of the mineral or sediment and n_e represents the effective porosity. In this manner, the batch and column K_ds can be easily compared. Although the column experiments have not yet reached saturation, retardation factors are presented below based on batch experiments. Once columns have sufficient breakthrough, a retardation factor will be calculated.

$$\tau = \frac{\int tC(t)dt}{\int C(t)dt} \quad \text{Eqn. 5}$$

$$V_{aqu} = \frac{\int VC(t)dV}{\int C(t)dV} - \frac{V_{spike}}{2} \quad \text{Eqn. 6}$$

$$R = 1 + \frac{K_d \times \rho_b}{n_e} \quad \text{Eqn. 7}$$

3.4 Instrumentation, Chemicals and Reagents

The following instruments and equipment will be used during the experiments and analysis:

- Soil characterization materials:
  - Fisher stainless steel sieve [No. 45, 100, 200 and pan]
  - Chempex Impact mortar and pestle, stainless steel [Cat. No. 850]
- pH electrode and meter [Thermo Scientific Orion Star A211 meter and Orion 9156BNWP electrode]
- Culebra dolomite (collected by Timothy Dittrich from WIPP)
- Equipment
  - Syringe pump [Kd Scientific Model 100 series]
  - Fraction collector [Gilson FC203B]
  - Inductively Coupled Plasma Mass Spectrometer (ICP-MS) [Agilent 7900]
- Column materials
  - 1/8” 27 NPT carbon pipe tap [Drillco cutting tools, 2700E108]
  - 1/8” Teflon fitting [Ipolymer, MCF12]
  - Teflon tubing [thin wall natural, PTFE#20, Item# 06417-31]

- 35 µm PEEK screen
- 20 gauge Teflon tubing
- 3-way luer lock
- Polypropylene syringe
- Silicone adhesive and Loctite marine epoxy

- Chemicals and Reagents
  - HCl, HNO_3 and NaOH, ACS reagent grade
  - NaCl, ACS reagent grade
  - $MgCl_2$, ACS reagent grade
  - Nd(III) and Am(III) stock solutions

4.0 Results

4.1 Dolomite Mineral Characterization

The Culebra sample (355 – 500 µm size fraction) was consistent with the dolomite mineral [$CaMg(CO_3)_2$] based on XRD and SEM-EDX as shown in Figures 5 and 6. Further, EDS analysis did not show significant impurities although analysis of more locations may be required to be statistically significant. BET surface area was measured at 1.6991 m^2/g.

Element	Wt%	At%
CK	10.55	19.97
OK	28.08	39.92
MgK	14.35	13.43
CaK	47.02	26.68

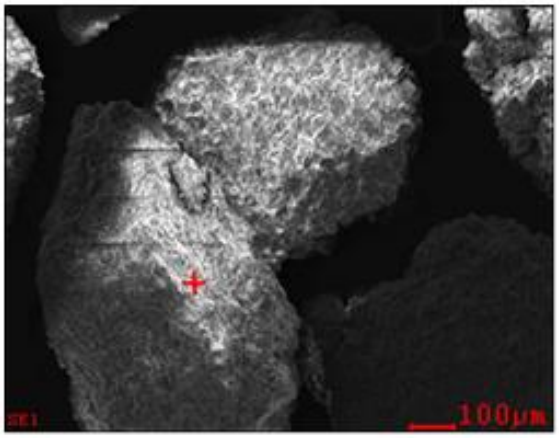

Figure 5. Representative SEM EDX analysis of Culebra formation, 355-500 µm size fraction, consistent with dolomite.

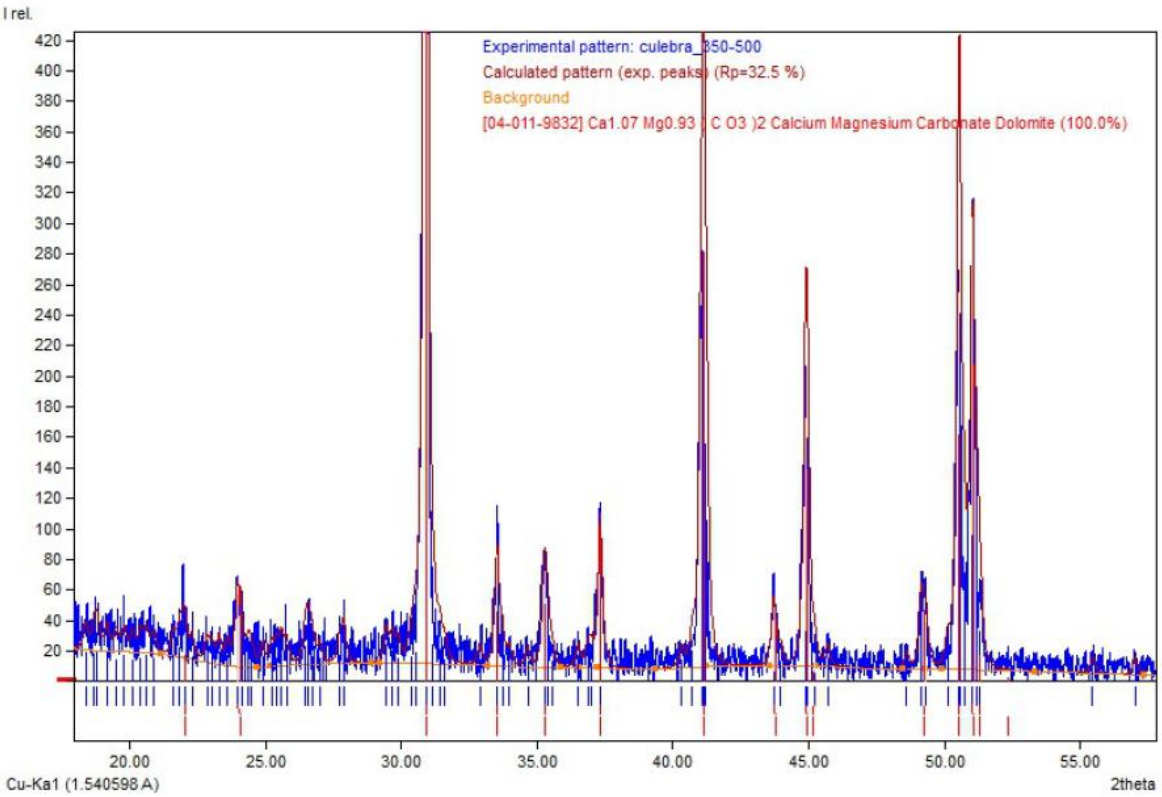

Figure 6. XRD spectra with reference spectra from Culebra formation, 355-500 µm size fraction for dolomite (Match! Software).

4.2 Batch Kinetics Results

Batch kinetics experiments were completed at 0.01, 0.1 and 1.0 M total ionic strength (3 mM $NaHCO_3$ + NaCl), 5 g/L dolomite, and 20 µg/L Nd (Figure 7 and 8). Figure 7 represents sorption with respect to time in terms of a K_d in mL/g while Figure 8 is normalized to the measured surface area of the 355 – 500 µm size fraction of dolomite used in these experiments (1.6991 m^2/g as measured by BET method). Samples were collected up to 3 days (4,320 minutes). However, preliminary data shows that sorption is strong and fast with equilibrium reached by 24 hours with sampling up to seven days without changes after the initial 24 hours.

Equilibrium K_d's are measured between 500 – 900 mL/g for 0.01, 0.1 and 1.0 M ionic strengths. Further, it should be noted that kinetics are similar for each of the different ionic strengths considered, although the highest ionic strengths have not yet been completed (2.0 and 5.0 M). Table 2 shows the equilibrium pH and pC_{H+} as determined using the corrections based on equation

1 and 2 in the Materials and Methods section as outlined previously (Borkowski, Lucchini et al. 2009).

Table 2. Summary of pH and pC_{H+} Values for Batch Sample Sets

	pH	pC_{H+}
1.0 M	8.29±0.08	8.41±0.38
0.1 M	8.64±0.08	8.59±0.38
0.01 M	8.67±0.11	8.60±0.39

Note: pC_{H+} corrections based on Borkowski et al. (2009) with error propagated from their fit with a linear model

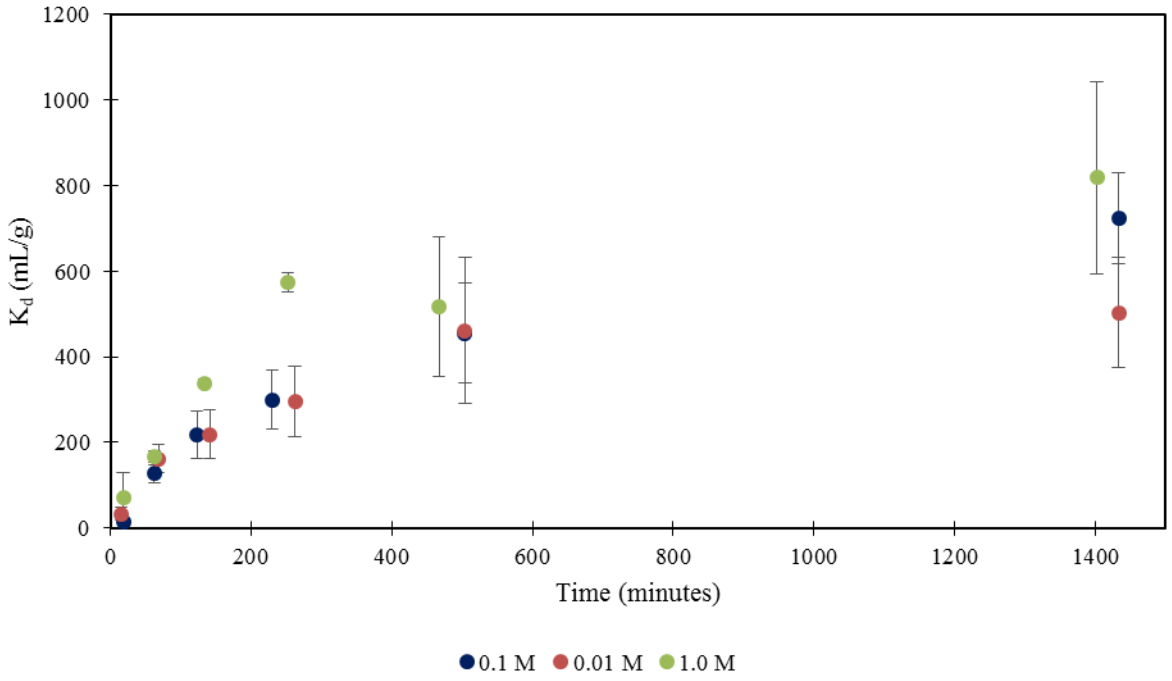

Figure 7. K_d (mL/g) partitioning of 20 µg/L Nd in the presence of 5 g/L dolomite with respect to time in 0.01, 0.1, and 1.0 M total ionic strength (NaCl + 0.003 M $NaHCO_3$).

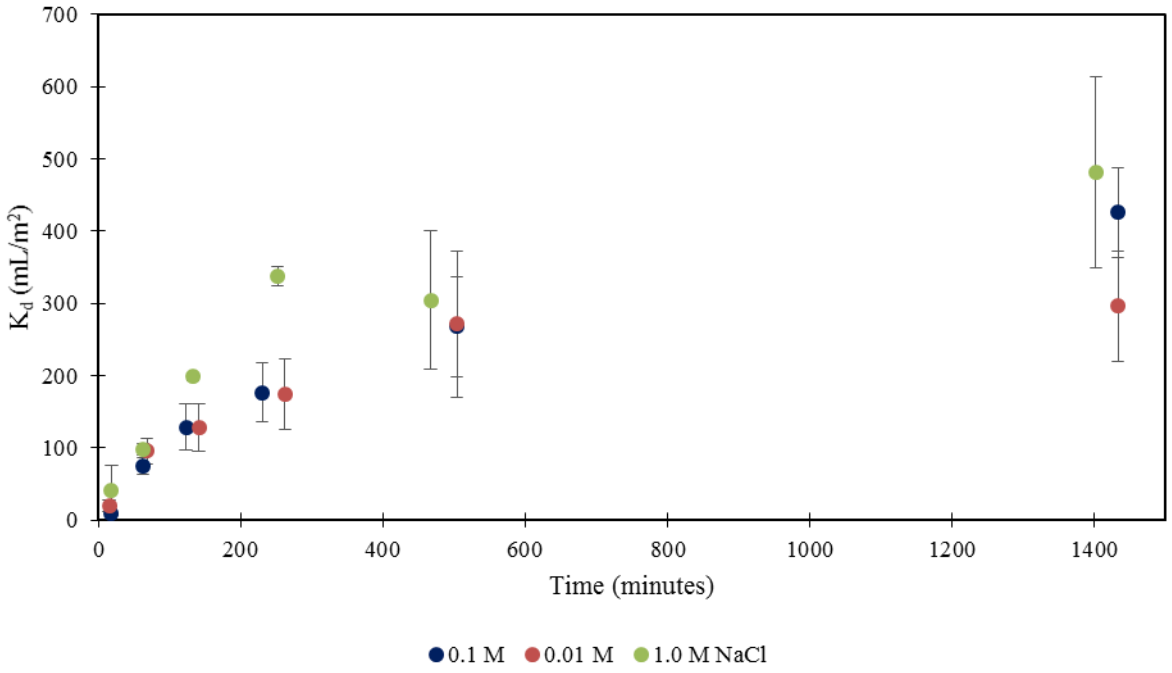

Figure 8. K_d (mL/m^2) partitioning of 20 µg/L Nd in the presence of 5 g/L dolomite with respect to time in 0.01, 0.1, and 1.0 M total ionic strength (NaCl + 0.003 M $NaHCO_3$).

The time dependent batch sorption data was fit with both first order and second order kinetic models as summarized in Table 3 below. The data was fit to 250 – 500 minutes as the reaction seemed to slow after this period and not follow either reaction model. However, the second order model appears to give the best fit for each of the datasets as shown by the R^2 correlation value in Table 3. Figures 9 – 14 show the model fits based on the plot of the linearized equation.

Table 3. Kinetic Model Equations and Fits for Batch Sorption Experiments

Kinetic model	General Equation	Plot	R^2 Correlation		
			0.01 M	0.1 M	1.0 M
First-order	$C_t = C_o e^{-k_1 t}$	$ln[C_t]\ vs.\ t$	0.8471	0.8535	0.9761
Second-order	$C_t = \frac{C_0}{1 + C_0 k_2 t}$	$\frac{1}{C_t}\ vs.\ t$	0.9475	0.9141	0.9971

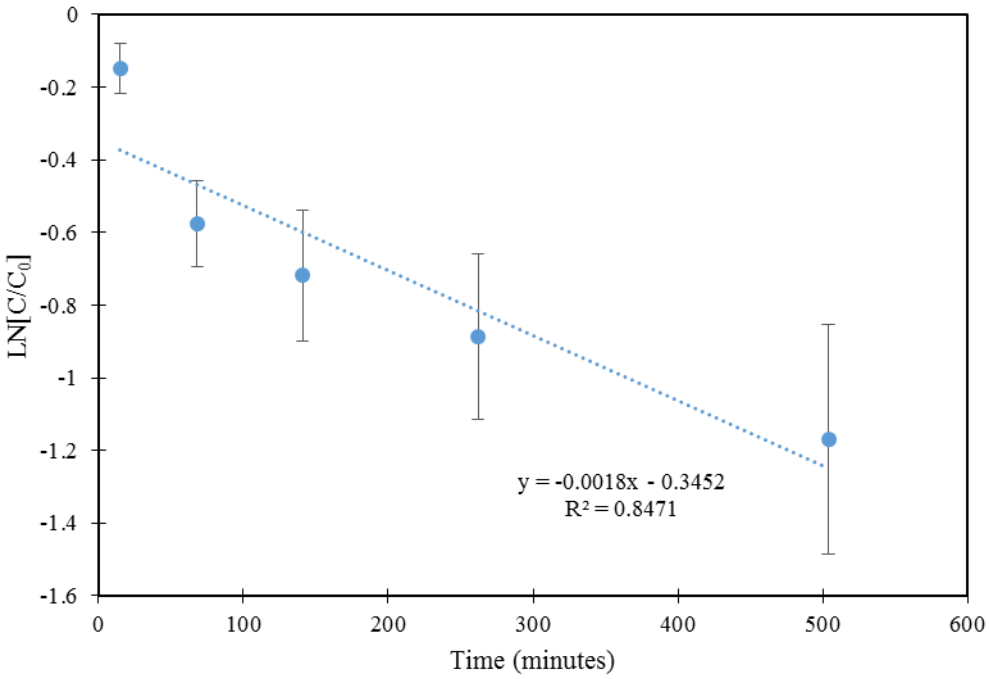

Figure 9. First order model fit for 0.01 M total ionic strength (3 mM $NaHCO_3$ + NaCl) for 20 µg/L Nd in the presence of 5 g/L dolomite.

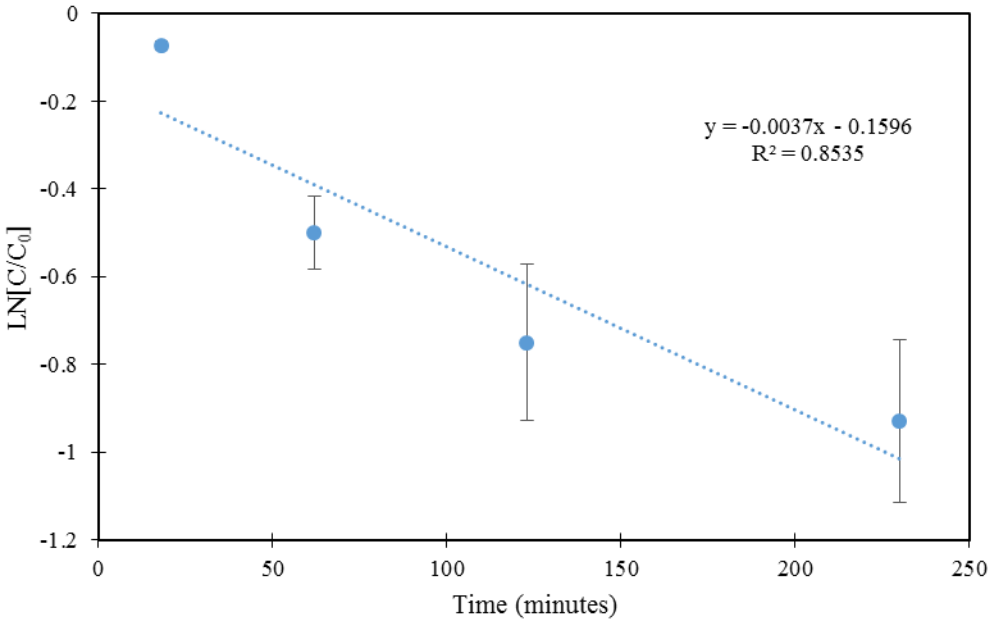

Figure 10. First order model fit for 0.1 M total ionic strength (3 mM $NaHCO_3$ + NaCl) for 20 µg/L Nd in the presence of 5 g/L dolomite.

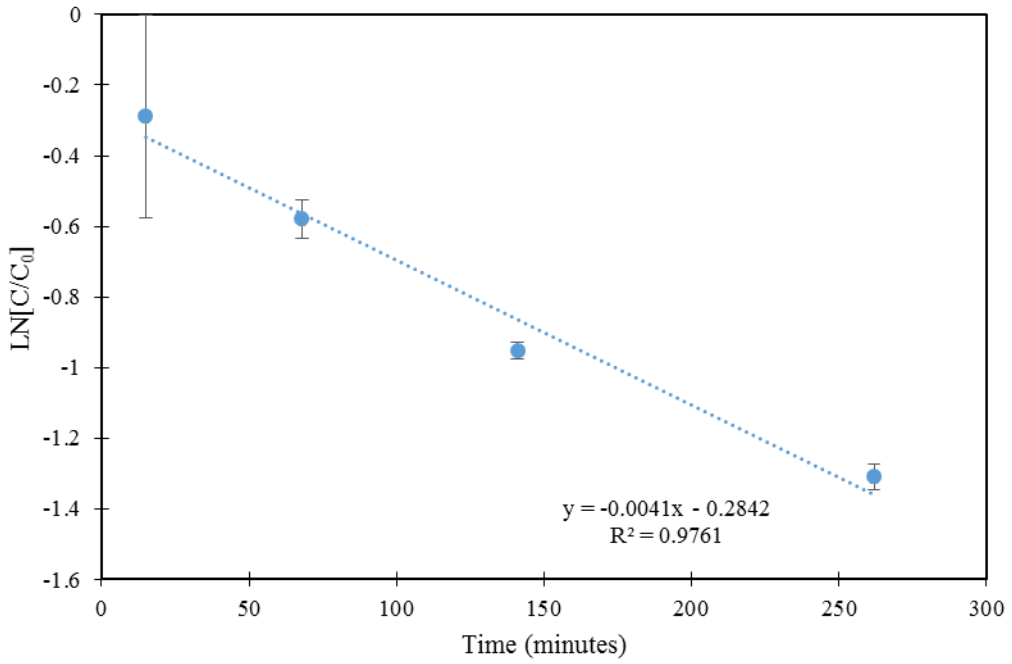

Figure 11. First order model fit for 1.0 M total ionic strength (3 mM $NaHCO_3$ + NaCl) for 20 µg/L Nd in the presence of 5 g/L dolomite.

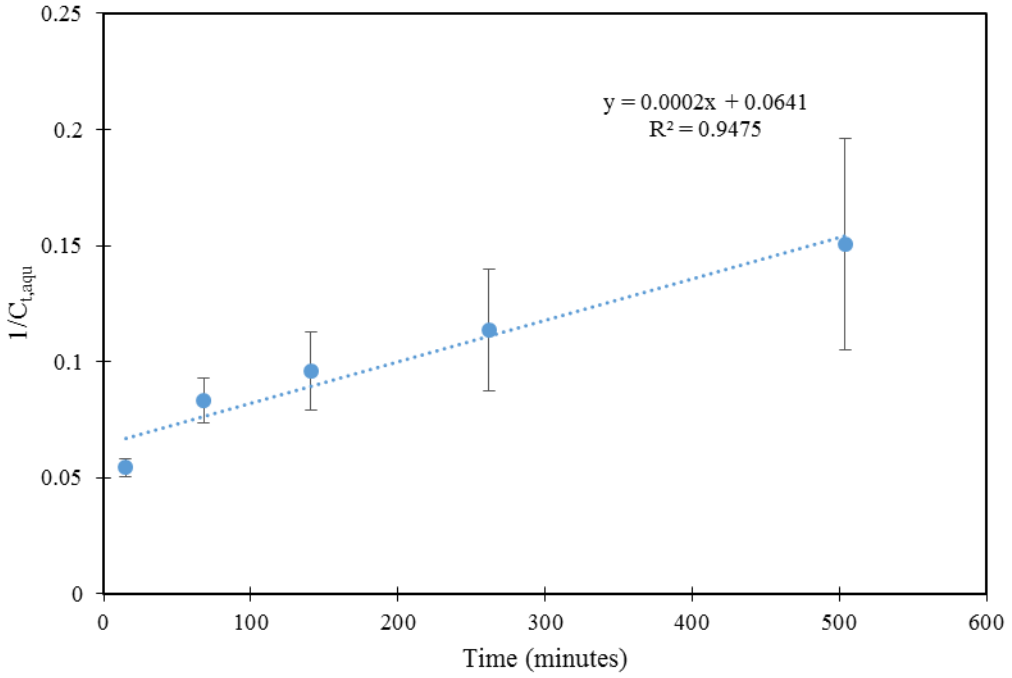

Figure 12. Second order model fit for 0.01 M total ionic strength (3 mM $NaHCO_3$ + NaCl) for 20 µg/L Nd in the presence of 5 g/L dolomite.

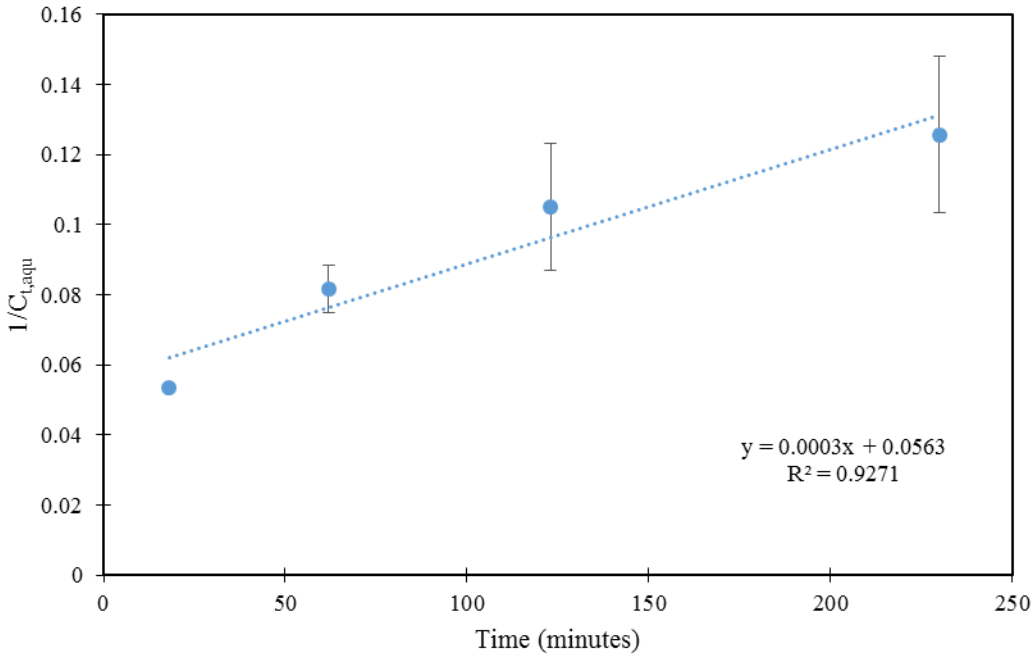

Figure 13. Second order model fit for 0.1 M total ionic strength (3 mM $NaHCO_3$ + NaCl) for 20 µg/L Nd in the presence of 5 g/L dolomite.

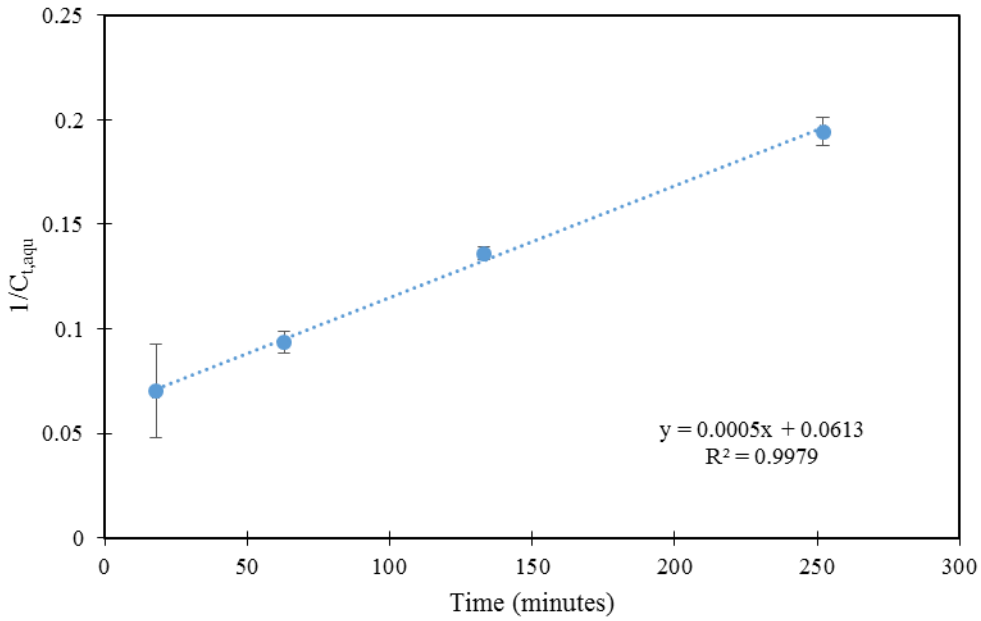

Figure 14. Second order model fit for 1.0 M total ionic strength (3 mM $NaHCO_3$ + NaCl) for 20 µg/L Nd in the presence of 5 g/L dolomite.

4.3 Column Experimental

4.3.1 0.01 M NaCl Column (Preliminary Testing)

The experimental conditions for the initial column were 100 µg/L Nd in 0.01 M NaCl and a target pH of 8.5. There was considerable fluctuation in the effluent pH (7.96±0.34). These pH fluctuations were likely due to the low buffering capacity of NaCl and disequilibrium with atmospheric carbonate. In order to stabilize the pH of the injection solutions, 3 mM $NaHCO_3$ was added to future experiments. This concentration of bicarbonate is close to the predicted concentration at pH 8.5 in equilibrium with atmospheric carbon dioxide.

In addition, there was some variability in stock measurements for Nd pulled from the syringes and bottles over time. Over the length of the experiments (approximately two weeks), the stock suspensions in bottles were measured at 84±9% of the initial and in syringes at 70±10%. Therefore, there were some losses of Nd due to sorption to walls and/or precipitation.

However, more significant losses were recorded following filtration through a 0.5 mL 30k MWCO filter (Amicon EMD Millipore) with recovery of ~20% of the initial Nd following filtration. Filtration of acidified Nd stock solutions was within error of the initial solutions. The filtration shows that Nd is either adsorbing to filter material, the filters are removing precipitated Nd or a mixture of both. However, to reduce possible precipitation, the stock solutions for future experiments were reduced to 20 µg/L Nd.

After running the preliminary column experiment for approximately three weeks (and nearly 800 pore volumes), the experiment was suspended. The breakthrough data is summarized in Figure 15 below. It should be noted that the steep drop in Nd breakthrough near 700 pore volumes is the point where injection of 100 µg/L Nd in 0.01 M NaCl was suspended and a desorption step using 0.01 M NaCl injection was begun (without Nd). However, significant desorption did not occur during injection of 0.01 M NaCl. Near 775 pore volumes, injection of 0.007 M NaCl + 0.003 M $NaHCO_3$ was begun and greater desorption of Nd occurred due to formation of Nd-carbonate species.

It is significant that approximately 15% of the Nd spike was present in the effluent for the majority of the column experiment. It is likely that these concentrations represent: (1) mobile Nd colloids, (2) Nd that did not have time to sorb due to sorption kinetics of Nd on dolomite and the short

retention time in the column (17 minutes), or (3) preferential flow within the column leading to significantly shorter retention times for a fraction of the flow. However, current work in ongoing to understand if the effluent concentrations may represent dissolved or colloidal Nd.

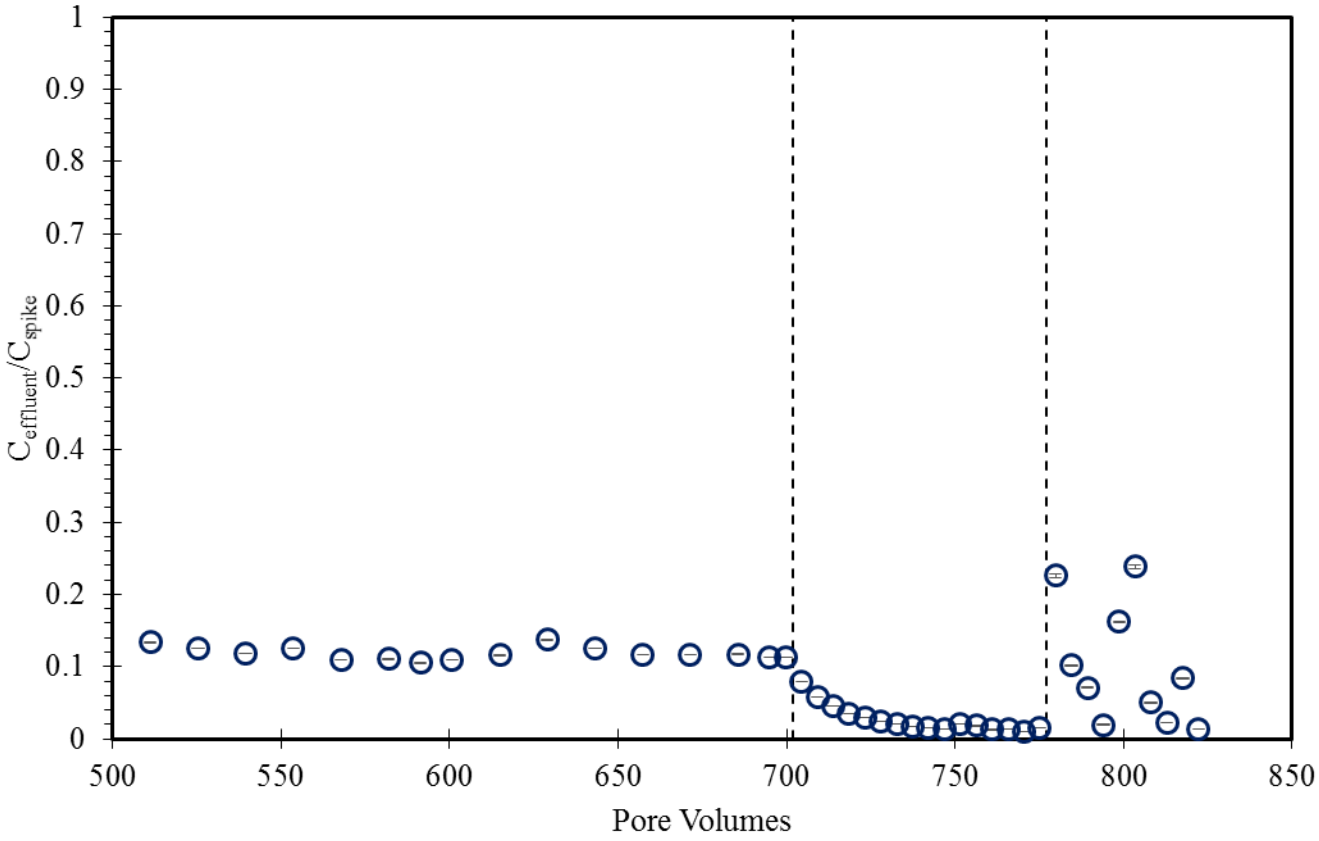

Figure 15. Breakthrough results from the preliminary column experiment [100 µg/L Nd, 0.01 M NaCl], Note: injection of 0.01 M NaCl without Nd was begun near 700 pore volumes and 0.007 M NaCl + 0.003 M $NaHCO_3$ near 775 pore volumes as shown by dotted lines.

4.3.2 0.1 M Total Ionic Strength Column

A long-term mini column with 0.1 M total ionic strength (3 mM $NaHCO_3$ + NaCl) and 20 µg/L Nd continuous injection at 1.5 mL/hr is currently in progress (Figure 16). More than 1900 pore volumes have been pushed through the column without saturation of the column. The column is 1 cm in length and contains approximately one gram of dolomite with a porosity of ~0.32. Therefore, if breakthrough had occurred at 1900 pore volumes, the K_d for Nd as calculated by the mini columns would be 200 mL/g. Therefore, based on the K_d's reported for the batch experiments (500 – 900 mL/g at equilibrium), we should not have reached the breakthrough point for the columns.

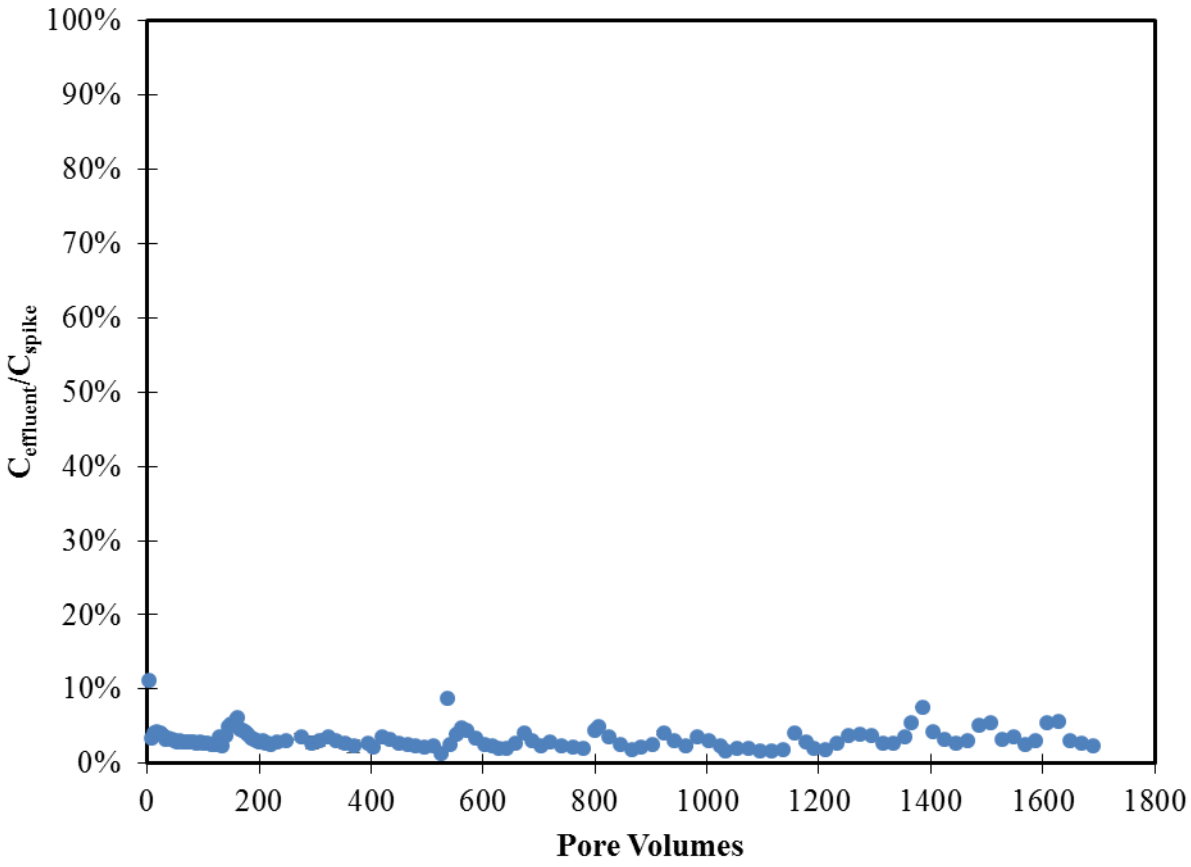

Figure 16. Continuous input of 20 µg/L Nd + 0.097 M NaCl + 0.003 M $NaHCO_3$ into mini column packed with dolomite at 1.5 mL/hr flow rate.

5.0 Conclusions

Although this work is still ongoing, significant improvements to the experimental methodology have been made as compared to the previous work conducted in the 1990's. Previous work measured sorption K_ds on the order of $10^{3.4}$ to 10^6 (Brush and Storz 1996, Brady, Papenguth et al. 1999, Perkins, Lucero et al. 1999). However, these experiments were limited in the pH range and ionic strength conditions evaluated and had precipitation and solubility issues. Therefore, the values reported in this work are expected to be more accurate.

Preliminary results show that sorption of Nd is likely greater than was assumed in the performance assessment process for the WIPP. The performance assessment models assumed a K_d of 20 – 400 mL/g (Brush and Storz 1996). Our preliminary batch experiments, albeit at lower ionic strength from 0.01 – 1.0 mol/L, predict sorption K_ds of 500 – 900 mL/g. The preliminary values in this

work show that the initial performance assessment models may have been conservative and likely overpredict transport of the trivalent actinides and lanthanides. However, it will be more appropriate to directly compare data at higher ionic strength.

Once breakthrough is achieved for the mini column experiments, this will provide a unique opportunity to compare both batch sorption and column experiments. This is an important endeavor as each of the types of experiments induce different experimental artefacts. In addition, this is the first dataset known to the author of this report that is investigating the kinetics of sorption of Nd to dolomite at variable ionic strengths. This will provide a better basic understanding of the effect of ionic strength on sorption of Nd as well as an idea of the kinetics of sorption to indicate whether kinetic models (as opposed to equilibrium K_d models) are necessary for the performance assessment process for the WIPP.

6.0 Future Work

Batch kinetics experiment will be conducted at 2 and 5 M total ionic strength [3 mM $NaHCO_3$ + NaCl] with measurements up to three days and will be analyzed for fit with the common kinetic sorption models for comparison with the 0.01 – 1.0 M ionic strength experiments. Further, batch experiments will be conducted at variable concentrations of dolomite and with repeated inputs of Nd to investigate the saturation point for comparison with mini column results. Additional kinetic sorption models will also be considered to determine best fit. The long-term mini column at 0.1 M total ionic strength will be continued by our LANL collaborators until breakthrough (i.e., saturation) has been reached. Additional column experiments will be run at FIU ARC for comparison (1 and 5 M total ionic strength). Finally, a model will be developed to describe the column breakthrough data utilizing PHREEQC.

7.0 References

1. BMWI (2008). Final Disposal of High-level Radioactive Waste in Germany: The Gorleben Repository Project. Gorleben, Germany, Federal Ministry of Economics and Technology.
2. Borkowski, M., J. F. Lucchini, M. Richmann and D. Reed (2009). Actinide (III) Solubility in WIPP Brine: Data Summary and Recommendations. L. A. N. Laboratory.
3. Brady, P. V., H. W. Papenguth and J. W. Kelly (1999). "Metal sorption to dolomite surfaces." Applied Geochemistry **14**(5): 569-579.

4. Brush, L. H. and L. J. Storz (1996). Revised Ranges and Probability Distributions of Kds for Dissolved Pu, Am, U, Th, and Np in the Culebra for the PA Calculations to Support the WIPP CCA. S. N. Laboratories. Albuquerque, NM.

5. Clark, M. M. (1996). Transport Modeling for Environmental Engineers and Scientists. New York, NY, John Wiley and Sons.

6. Dittrich, T. M. and P. W. Reimus (2015). "Uranium transport in a crushed granodiorite: Experiments and reactive transport modeling." Journal of Contaminant Hydrology **175**: 44-59.

7. Dittrich, T. M., S. D. Ware and P. W. Reimus (2016). Mini-columns for Conducting Breakthrough Experiments: Design and Construction. U. S. D. O. o. N. E. F. C. Technologies. Los Alamos, NM, Los Alamos National Laboratory.

8. Lucchini, J. F., M. Borkowski, H. M. Khaing, M. Richmann, J. S. Swanson, K. A. Simmona and D. Reed (2014). WIPP Actinide-Relevant Brine Chemistry. Carlsbad, NM, Los Alamos National Laboratory.

9. Meigs, L. C., R. L. Beauheim, J. T. McCord, Y. M. Tsang and R. Haggerty (1997). Design, modelling and current interpretations of the H-19 and H-11 tracer tests at the WIPP site. Field Tracer Experiments: Role in the Prediction of Radionuclide Migration. Cologne, Germany, Nuclear Energy Agency.

10. Perkins, W. G., D. A. Lucero and G. O. Brown (1999). Column Experiments for Radionuclide Adsorption Studies of the Culebra Dolomite: Retardation Parameter Estimation for Non-Eluted Actinide Species. S. N. Laboratories. Albuquerque, NM**:** 163.

11. Rai, D., A. R. Felmy, S. P. Juracich and L. F. Rao (1995). Estimating the Hydrogen Ion Concentration in Concentrated NaCl and Na2SO4 Electrolytes. S. N. Laboratories. Albuquerque, NM, Sandia National Lab.

12. Spiegel (2010) "Germany's Endless Search for a Nuclear Waste Dump." Spiegel Online International.

13. U.S.DOE (1995). Inventory WIPP Baseline Inventory Report. U. S. D. o. Energy. Carlsbad, NM.

14. U.S.DOE (1996). Title 40 CFR Part 191 Compliance Certification Application for the Waste Isolation Pilot Plant. U. S. D. o. Energy. Carlsbad, NM, Carlsbad Area Office.

15. U.S.EPA (1993). 40 CFR Part 191 Environmental Radiation Protection Standards for the Management and Disposal of Spent Nuclear Fuel, High-Level and Transuranic Radioactive Wastes; Final Rule. Federal Register. **58**.

16. Zavarin, M., S. K. Roberts, N. Hakem, A. M. Sawvel and A. B. Kersting (2005). "Eu(III), Sm(III), Np(V), Pu(V), and Pu(IV) sorption to calcite." Radiochimica Acta **93**: 93-102.